International Journal of Heat and Mass Transfer 51 (2008) 5662–5670

Contents lists available at ScienceDirect

International Journal of Heat and Mass Transfer

journal homepage: www.elsevier.com/locate/ijhmt

Targeted brain hypothermia induced by an interstitial cooling device in the rat neck: Experimental study and model validation

Yunjian Wang [a], Liang Zhu [a,*], Axel J. Rosengart [b]

[a] Department of Mechanical Engineering, University of Maryland Baltimore County, 1000 Hilltop Circle, Baltimore, MD 21250, United States
[b] Neuroscience Critical Care, New York Presbyterian Hospital, New York, NY, United States

ARTICLE INFO

Article history:
Received 21 November 2007
Received in revised form 4 April 2008
Available online 12 June 2008

Keywords:
Brain hypothermia
Ischemic brain injury
Interstitial cooling
Rat
Surgery

ABSTRACT

Targeted brain hypothermia has the potential to prevent cerebral ischemia injury during open heart and neck surgeries or after traumatic head injury. In this study, *in vivo* experiments were performed to test the performance of a newly developed cooling device in an inexpensive animal model. Rat brain hypothermia was induced by inserting an interstitial cooling device in the rat neck muscle and placing the device on the common carotid artery to cool the arterial blood supplied to the brain. Coolant was circulating inside the cooling device to achieve either mild or moderate temperature reductions at the surface of the device. Temperatures were measured inside the rat brain tissue, as well as on the head skin surface. For the mild cooling (cooling device surface temperature was 18.7 ± 4.5 °C), the temperature reductions were 2.2 ± 0.6 °C, 2.1 ± 0.6 °C, 1.9 ± 0.6 °C and 1.6 ± 0.9 °C at sites of brain-5 mm, brain-2 mm, skull, and scalp, respectively. After the surface temperature was further decreased to 12.8 ± 2.8 °C (moderate cooling), the temperature reduction in the head increased more than 85% to 3.7 ± 3.2 °C, 3.7 ± 3.0 °C, 3.3 ± 2.5 °C and 2.5 ± 1.0 °C, respectively. The experimental data were also used to validate a previously developed theoretical model for humans. Experimentally measured geometrical and physiological parameters of the rat neck and brain were substituted into the scaled-down theoretical model to simulate the temperature distribution in the rat neck and brain. The theoretically predicted brain temperatures showed a good agreement with the experiment data. We believe that this study is the first step in developing a reliable cooling device to achieve fast cooling and to control rewarming in future clinical studies and to benefit a large patient population.

1. Introduction

Neuroprotection, that is, reducing the impact of brain injury either prior to or after the occurrence of a damaging insult has the potential to greatly improve the mortality and morbidity of patients suffering from a wide variety of brain injuries. Currently, the most reliable and clinically useful neuroprotectant is cooling of the brain; for example, initiated prior to high-risk, complex cardiothoracic surgery which employs cardiopulmonary arrest and/or bypass, and hence, exposes the neural tissue to extended periods of cerebral perfusion standstill. The need to medically protect the brain in these settings has been addressed in several published investigations. A multicenter study by Roach et al. [1] reported that more than 6% of patients suffered neurological adverse events after coronary artery bypass surgery, a common procedure of revascularization of the blood supply of the heart after myocardial infarction. More subtle but equally important neuropsychological deficits or impairments in cognition were detected in more than 20% of bypass patients months after surgery [2]. The mechanism leading to brain ischemia during such surgeries often is a combinatory effect from global brain hypoperfusion, direct embolization of atherosclerotic material with cumulative occlusions of small brain arteries [3], and temporary large vessels, i.e., carotid artery. Often, these occlusions are necessitated by the surgery [4].

A significant body of literature demonstrates that even mild reductions in brain temperature, i.e., by 1 or 2 °C, are effective to reduce ongoing secondary damage in the acutely injured brain. The palliative effects directly translate into clinical benefits, mainly reductions in death and disability after brain injury. Brain hypothermia reduces tissue oxygen demands [5] and ameliorates numerous deleterious cellular biochemical mechanisms, including calcium shift, excitotoxicity, lipid peroxidation and other free radical reactions, DNA damage, and inflammation [6]. In particular, hypothermia initiated prior to or immediately after the onset of the damaging event provides potent, dose-(temperature-)related and long-lasting neuroprotection as evidenced in many experimental studies [7]. Conversely, an elevated brain temperature of

* Corresponding author. Tel.: +1 410 455 3332; fax: +1 410 455 1052.
E-mail address: zliang@umbc.edu (L. Zhu).

0017-9310/$ - see front matter © 2008 Elsevier Ltd. All rights reserved.
doi:10.1016/j.ijheatmasstransfer.2008.04.042

Nomenclature

c	Specific heat (J kg^{-1} K^{-1})
d	Distance defined in Fig. 3 (m)
e	Distance defined in Fig. 3 (m)
k	Thermal conductivity (W m^{-1} K^{-1})
h	Heat transfer coefficient (W m^{-2} K^{-1})
L	Length of the neck cylinder (m)
M	Mass (kg)
q_{loss}	Total heat loss from the arterial blood to the device per unit time (W)
q_m	Local metabolic heat generation rate (W m^{-3})
Q	Volumetric flow rate (m^3 s^{-1})
r	Radial distance from the center of the artery in cylindrical coordinates (m)
R	Radial distance from the center of the neck cylinder in cylindrical coordinates (m)
t	Time (s)
T	Temperature (°C or K)
z	Axial distance in cylindrical coordinates (m)

Greek symbols

ρ	Density (kg/m^3)
θ	Polar angle in cylindrical coordinates
ω	Local volumetric blood perfusion rate per unit volume of tissue (s^{-1})

Subscripts

a	Artery
b	Blood
bt	Brain
n	Neck
t	Tissue

only 1–2 °C strikingly worsens neuronal injury in experimental settings and has a clinically proven, negative impact on patient outcome [8].

There are two conceptual approaches to reduce brain temperature but unfortunately, only one, systemic cooling, has achieved clinical utility. Systemic cooling induces brain hypothermia by reducing the temperature of the whole body, commonly via venous blood cooling. It is an effective approach in brain injury as approximately 20% of the cardiac output (and hence, cooled blood) is delivered to the brain and modern clinical care can utilize intravascular cooling catheters to achieve powerful, rapid, and constant hypothermia induction. However, adverse events from whole body cooling predominate and curtail its clinical usefulness in a cooling depth- and time-dependent manner leading to a reversal of the benefit-risk ratio [6,9]. The second approach to brain cooling is targeted hypothermia in which the brain is selectively cooled while the rest of the body is kept euthermic. The opportunity to cool the brain selectively, thereby avoiding the main adverse events of systemic cooling such as infections and sepsis, blood clotting abnormalities, and heart and lung failure, is of great clinical and biomedical engineering interest. Employing a historically well-known method of external head cooling with ice packs or cooling wraps has led to clinical use of cooling helmets in brain-injured neonates. Recent theoretical [10,11], animal [12–14], and clinical [15] studies have demonstrated that external head cooling will not penetrate beyond the brain gray (upper surface) matter. Some of the more invasive targeted brain cooling approaches under investigation with unknown clinical usefulness include nasopharyngeal cooling, direct catheter cooling [16], and intra-carotid flushing with coolant.

An alternative approach to achieve fast and uniform temperature reduction throughout most of the brain tissue is to reduce the temperature of the carotid arteries in the neck as these vessels are responsible for about 80% of the total brain perfusion. However, a previous theoretical investigation by the author [17] delineated the ineffectiveness to reduce brain temperature via applying surface neck cooling of the carotid arteries. In contrast, if an appropriately designed cooling device is inserted safely under the skin and in physical contact with the common carotid artery (CCA), more effective brain cooling could possibly be achieved by reducing the thermal resistance between the cooling device and the artery. A previous simulation of the human neck and head using this cooling approach [18] demonstrated the theoretical feasibility of inducing at least a 3 °C temperature drop along each CCA. However, the theoretical model needs validation before the cooling device can be used in clinical studies.

Animal experiments are usually performed to test any cooling device and to measure the temperature reduction in the brain tissue. An approach to the development of a model of this cooling methodology for humans is to begin with small animal studies. A comparison of the experimentally measured data on small animals with the theoretical model for animals can be used to validate the theoretical model for the animal. In most of the animal studies of a medical device, model validation is necessary to assess the accuracy of the theoretical model in handling complicated and realistic structures such as the brain or neck. Once the theoretical model is validated in small rodents, experimental studies can be conducted on large animals. This approach provides confidence that the cooling capacity applied to human anatomy is accurate and reliable before the device can be used in future clinical studies.

Based on the encouraging results obtained from our previous theoretical work [18], we now utilized *in vivo* rodent experiments to report on brain hypothermia induction and distribution during direct CCA cooling and compare the obtained results to our previously obtained simulations. A compact neck cooling device, made from flexible two-dimensional cooling sheets, was designed and brought in direct physical contact with both common carotid arteries of anesthetized rats. The temperature distribution in the brain tissue was measured and the effects of variations in coolant temperature were evaluated. In our analyses, we included the detailed vascular geometry and blood flow rates of the test animals and, based on the obtained data, we extended and validated the previously reported theoretical model to accurately simulate the temperature fields in the neck and brain of the animal.

2. Materials and methods

In vivo experiments were performed to measure the transient brain temperature distributions and to determine the temperature reductions at various brain tissue locations after inserting a specifically designed cooling device with close proximity to the CCA into the neck of anesthetized rats. The feasibility of inducing hypothermia via direct CCA cooling was *a priori* defined as brain hypothermia (34 °C) within 40 min of cooling.

Six Sprague-Dawley rats (456 ± 26 g, males) provided by Charles River Laboratory (Wilmington, MA) were used. At the beginning of the experiment, each rat was anesthetized and maintained in sedation with intraperitoneal injections (i.p.) of sodium

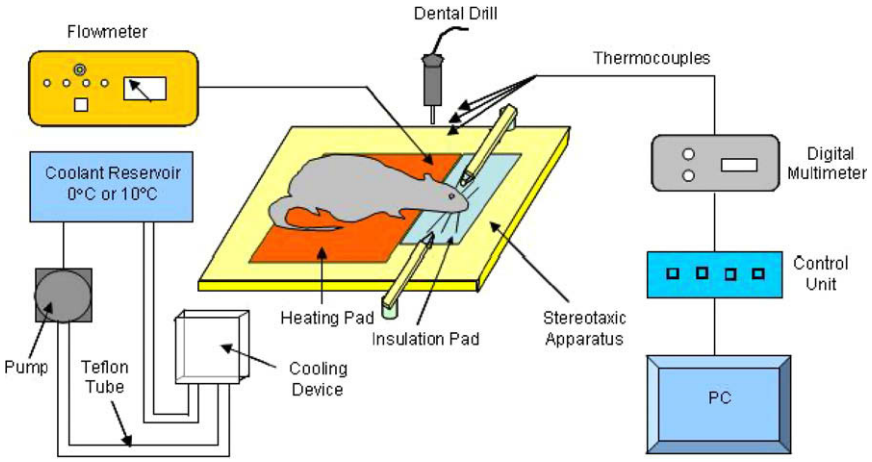

Fig. 1. Experimental setup of the animal study and the schematic diagram of the cooling device (enlarged).

pentobarbital (40 mg/kg) and placed on a water-jacketed heating pad to maintain normal core temperatures (~37 °C) as monitored by the rectal temperature (Fig. 1). The neck cooling device was made from a flat sheet of plastic (length = 1.0 cm, width = 1.0 cm) that received circulating coolant (water) from a temperature-controlled water reservoir while the coolant flow rate through the sheets was controlled by a high resolution peristaltic pump (World Precision Instruments, Inc., Sarasota, Florida). The CCAs were exposed on both sides of the lower neck through a 2–3 cm midline neck incision and specific precautions were taken not to damage other surrounding neck structures, i.e., nerves. The volumetric blood flow rate in the left common carotid artery, Q, was recorded by a T106/T206 Animal Research Flowmeter (Transonic® System Inc., New York) after suture attachment of the 0.7 mm V-shaped flow probe around the very proximal CCA to avoid proximity to the adjacent jugular vein. Teflon tubes (~0.5 mm I.D.) of the cooling device were connected to the pump and two thermocouples were attached to the inner surface of the device. The skin remained closed during the experiments.

The head was fixed in a stereotactic frame (Stoelting Inc., Wood Dale, IL). After retraction of the scalp, a craniotomy was made over the left and right parietal cortices along the coronal and inter-parietal suture margins. With a small drill bit (0.4 mm dia.), a small burr hole was carefully made 3 mm lateral and 2 mm posterior to the bregma employing a continuous of 0.9% saline drip to prevent heat injury of the underlying cortex. Three fine thermocouples (50 μm dia. O.D. wire) were bundled together but remained 3 mm apart from each other and then inserted through the burr hole to various predesignated positions. As shown in Fig. 2, one thermocouple was placed between the skull and scalp and the remaining were positioned at 2 mm and 5 mm depths into the brain. The stereotactic head frame greatly supported precise burr hole drilling, insertion of the thermocouples, and accuracy of continuous temperature recordings throughout the experiment. The calvarium was sealed around the wires with bone wax (Stoelting Inc., Wood Dale, IL), and the skin was closed. Several K-type thermocouples were placed on various locations at the head surface to monitor skin temperatures.

The cooling devices, placed on both common carotid arteries, delineated the effects of various cooling temperatures on the cooling capacity and the experimental group ($n = 6$) studied. Each animal was first exposed to a device temperature at 18.7 ± 4.5 °C and then, after recovery to baseline temperature, cooled in a subsequent step to 12.8 ± 2.8 °C. The respective coolant reservoir temperatures were kept at 10.0 ± 0.8 °C and 0.0 ± 0.6 °C. The coolant flow rate was 60 ml min^{-1}. All the data were recorded and stored using the LabView® program on a personal computer. The temperatures were recorded every ten seconds. The experimental protocol included the following steps: (1) The baseline temperatures were measured and recorded for 30 min after completion of the surgery. (2) The first, mild cooling, was introduced for 40 min to achieve a cooling device temperature of ~18.7 °C. (3) After this first cooling period, the coolant was stopped for 30 min during which time period all temperature sites continued recording the spontaneous temperature recovery in the animal, which was otherwise kept euthermic. (4) The second, moderate cooling period (~12.8 °C on the device surface) was initiated and maintained for 40 min. (5) Following step (4), spontaneous temperature recovery (step 3) was again recorded.

At the end of the experiment, the rat was euthanized with sodium pentobarbital (150 mg/kg, i.p.). The brain was sectioned to validate the correct temperature sensor positioning and to inspect for adverse effects (i.e., hematoma, etc.) related to the surgery, and the thicknesses of scalp, bone, and brain tissue were measured. The neck was reopened to delineate the positioning and physical relationship of the common carotid arteries. The sizes of the common, internal and external carotid arteries, and the internal and external jugular veins were measured by means of a Nikon® SMZ800 dissection microscope.

Blood flow rate and temperatures for each trial were analyzed and expressed as a mean ± SD. Differences among the mean values

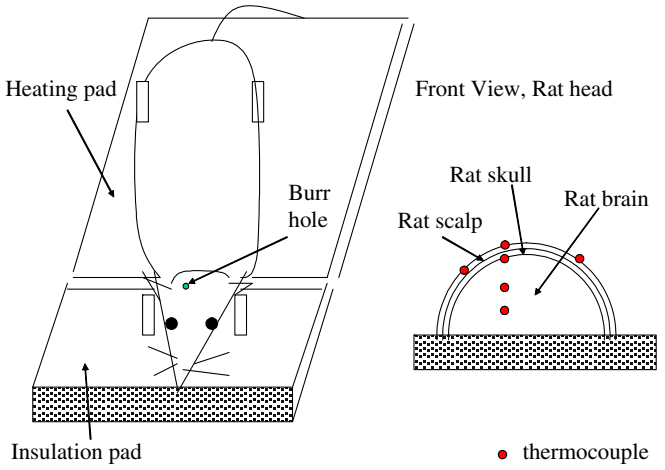

Fig. 2. Schematic diagram of the *in vivo* experiment on the rats during targeted brain cooling and the temperature sites in the rat head.

were determined by one-way repeated measures ANOVA. The *post hoc* comparisons of the temperatures between the baseline measurement and cooling or rewarming were performed by Student's *t*-test. Significance was evaluated at the 5% confidence level.

3. Theoretical model

The previously developed theoretical model for the human neck and brain [18] was scaled down for the anatomy of the rat neck and brain. Parameters required for modeling the temperature fields of the rat neck and brain include the locations and sizes of the major blood vessels in the neck, the size of the neck, the blood flow rate of the common carotid artery, and the head dimensions. All the parameters measured in the animal experiments and thermal properties obtained from the literature were incorporated into the theoretical model to simulate the temperature distribution. Temperature predictions in the rat brain were then compared with the experimentally measured data. The validity of the theoretical model can be confirmed when the theoretically predicted temperatures agree with the experimental results.

In this study, a three-dimensional model of the rat neck (Fig. 3) and head (Fig. 4) with embedded common carotid arteries was employed to simulate the tissue temperature reductions induced by the cooling device. We ignored the influence of other neck vessels on the CCA temperatures as vessel-to-vessel thermal interactions are negligible for vessels not in close proximity [17,19]. Fig. 3 gives the schematic diagram of the rat neck where the common carotid arteries are modeled as two straight tubes on either side of the neck cylinder with the respective the cooling devices in form of a rectangular column. The common carotid artery usually gives no bifurcations before it bifurcates into the internal and external carotid arteries. The small blood vessels, that provide nutrients to the muscle tissue of the neck, mainly come from the external carotid artery. The external carotid artery also provides blood supply to the superficial head and face regions. Because of the small nutrient need in the neck region, only a very tiny portion of the blood flow in the common carotid artery is used to supply nutrients to the neck muscle.

A mathematical model for the neck temperature field was formulated based on the structures delineated in Fig. 3. One could write the conservation energy equations for the arteries and tissue in cylindrical coordinates (inside the arteries – r_a, θ_a, z; inside the tissue cylinder – R, θ, z) as follows:

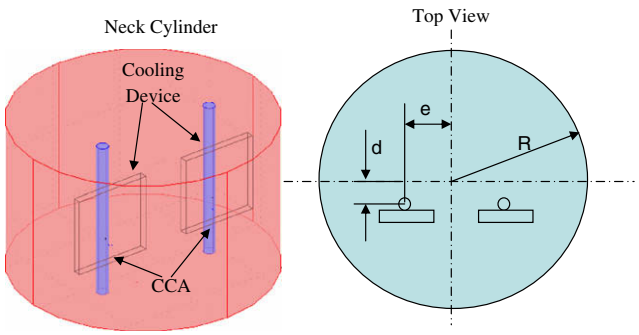

Fig. 3. Geometry of the rat neck region with two common carotid arteries embedded in tissue and the cooling device. (a) Three-dimensional view and (b) top view.

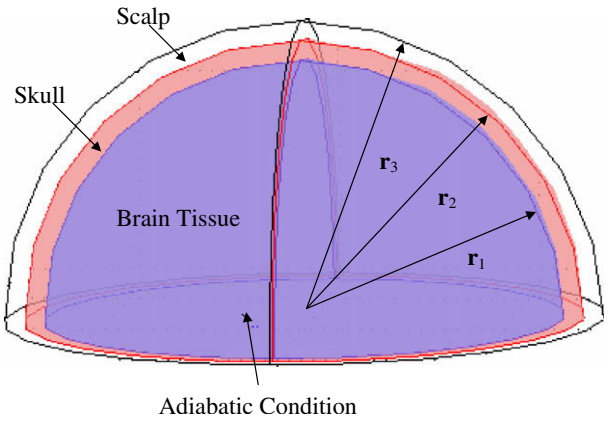

Fig. 4. Simplified geometry of the rat head consisting of the scalp, skull, and brain tissue.

$$\text{artery}: \rho_b c_b \frac{\partial T_{ai}}{\partial t} = k_b \left\{ \left[\frac{1}{r_{ai}} \frac{\partial}{\partial r_{ai}} \left(r_{ai} \frac{\partial T_{ai}}{\partial r_{ai}} \right) \right] + \frac{1}{r_{ai}^2} \frac{\partial^2 T_{ai}}{\partial \theta_{ai}^2} + \frac{\partial^2 T_{ai}}{\partial z^2} \right\} - \rho_b c_b u_{ai} \frac{\partial T_{ai}}{\partial z} \quad r_{ai} \leqslant a_{ai}, 0 \leqslant z \leqslant L, \ \ i = 1,2 \tag{1}$$

$$\text{tissue}: \rho_t c_t \frac{\partial T_t}{\partial t} = k_t \left\{ \left[\frac{1}{R} \frac{\partial}{\partial R} \left(R \frac{\partial T_t}{\partial R} \right) \right] + \frac{1}{R^2} \frac{\partial^2 T_t}{\partial \theta^2} + \frac{\partial^2 T_t}{\partial z^2} \right\} + \rho_b c_b \omega_n (T_{a,\text{neck}} - T_t) \quad R \leqslant R_t, r_{ai} > a_{ai}, 0 \leqslant z \leqslant L, \ \ i = 1,2 \tag{2}$$

where subscript i denotes the prescribed number of the arteries, subscriptions a, b, t, n refer to artery, blood, tissue, and neck, respectively, a_{ai} and R_t are the radius of the blood vessel and neck tissue cylinder, respectively, k is thermal conductivity, ρ is density, c is specific heat, and u_a is the average blood flow velocity in the common carotid artery. The temperature distribution along the carotid artery was determined by heat conduction to the surrounding tissue and to the cooling device (the first term on the right side of Eq. (1)) and heat convection due to blood flow (the second term on the right side of Eq. (1)). In the neck tissue cylinder, temperature field in the neck is a combination of heat conduction and blood flow effect in the neck tissue. As suggested by the Pennes bioheat equation [20], local blood perfusion in the neck tissue or the thermal effect of those small blood vessels acts as a heat source to warm the tissue. Its strength is directly proportional to the local blood perfusion rate, ω_n (s^{-1}). $T_{a,\ neck}$ is the local arterial temperature and is assumed equal to the body temperature measured by the experiments.

We assumed that the neck surface is subject to a room temperature of T_{room} measured as 25 °C and a heat transfer coefficient h (8 W m^{-2} K^{-1}), which accounts for a combination of natural convection and radiation heat transfer to the surroundings. The effect of the cooling device was modeled as a boundary condition of a uniform temperature at the outer surface of the device ($T_{cooling}$ = 18.7 °C or 12.8 °C). The boundary condition at the bottom surface of the cylinder was prescribed as the body temperature. In our previous study [18] we showed that the top region of the neck, that is, the interface with the head, has a temperature reduction due to interstitial cooling in the neck. We also found that the

calculated temperature decays along the common carotid artery were not very sensitive to the thermal condition of this interface. Therefore, for simplicity, the boundary condition at this interface was prescribed as an adiabatic condition.

Similar to our previous theoretical model of the human head [10,11], the rat head was modeled as a spherical structure consisting of scalp, skull, and brain tissue. The blood flow effect in each structure in the head was modeled as a Pennes perfusion source term. For any tissue structure (scalp, skull, or brain tissue), the Pennes bioheat equation was written as

$$\rho_{\mathrm{scalp,skull,bt}} c_{\mathrm{scalp,skull,bt}} \frac{\partial T_{\mathrm{scalp,skull,bt}}}{\partial t} = k_{\mathrm{scalp,skull,bt}} \nabla^2 T_{\mathrm{scalp,skull,bt}} + \rho_{\mathrm{b}} c_{\mathrm{b}} \omega_{\mathrm{scalp,skull,bt}} (T_{\mathrm{bm}} - T_{\mathrm{scalp,skull,bt}}) + q_{\mathrm{m}} \quad (3)$$

where q_{m} is the local metabolic heat generation rate, and T_{bm} is the temperature of the arterial blood supplied to the brain tissue. Since the cooling device in the neck reduces the temperature of the blood in the common carotid arteries, it can be expected that the blood temperature at the terminus of the carotid artery would be lower than the body temperature. In this study, T_{bm} was the average temperature of the blood in the common carotid artery calculated by solving Eq. (1). At the bottom of the head, an adiabatic condition was prescribed since an insulation pad is put under the head of the rat during the experiment, as shown in Fig. 2.

Table 1
Baseline parameter measured in the animal experiments ($n = 6$)

Rat weight (g)	Brain mass (g)	Blood flow rate (ml min^{-1})	Rectal temperature (°C)
456 ± 26	2.06 ± 0.19	4.4 ± 2.2	38.3 ± 0.4

Temperature fields in the neck, blood vessel and head were solved using the finite element method. All the finite element calculations including the mesh generation and solving were performed on FEMLAB 3.1 operated on a Pentium IV processor of 2.79 GHz speed, using 1 GB of memory under a Windows XP SP2 Professional Operating System. The numerical model was obtained by applying the Galerkian formulation of Eqs. (1)–(3). The total number of tetrahedral elements of the finite element mesh in the neck was around 81103. Mesh independency was checked by increasing the number of elements in the artery by 20% over the current mesh; the finer mesh induced less than 1% global difference in the temperature field. The mesh was not further refined since the finer mesh resolution has reached the maximal capacity supported by the internal memory of 1 GB in the computer of our laboratory.

4. Results

Table 1 describes the baseline data measured in the experiments ($n = 6$). The weight of brain tissue was 2.1 ± 0.2 g and the average blood flow rate in each common carotid artery was 4.4 ± 2.2 ml min^{-1}, a similar value as found in a previous study [14]. The average baseline rectal temperature, 38.3 ± 0.4 °C, was similar to the naturally occurring rat body temperatures.

Fig. 5 delineates the recorded temperatures at different locations at different stages, including the baseline (precooling), the mild cooling, the first recovery, the moderate cooling, and the second recovery stages. The temperature field of the brain tissue was relatively uniform before the initiation of the cooling and the temperature decreases slightly towards the skin surface (from 38.3 °C to 36 °C). For the mild cooling (cooling device surface temperature is 18.7 ± 4.5 °C), the temperature drops were 2.2 ± 0.6 °C, 2.1 ± 0.6 °C, 1.9 ± 0.6 °C and 1.6 ± 0.9 °C at sites of brain-5 mm, brain-2 mm, skull and scalp, respectively. For the moderate cooling (cool-

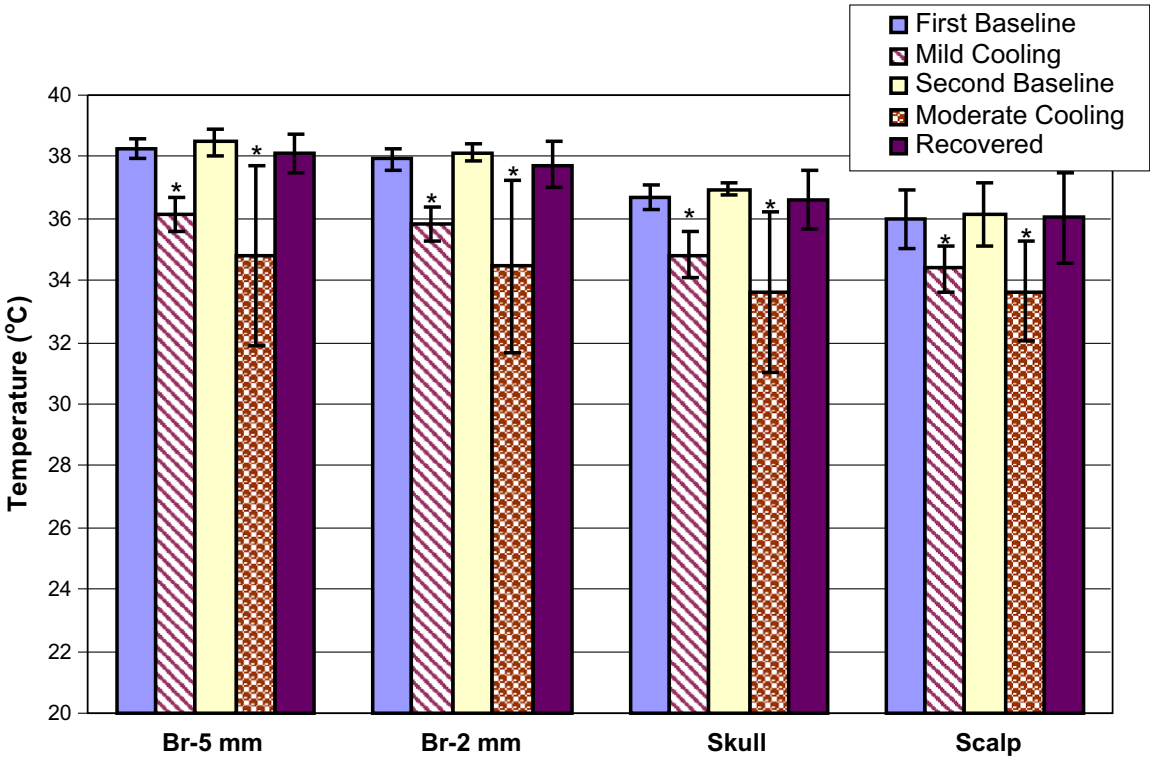

Fig. 5. The tissue temperatures at different locations for the baseline, mild cooling, the first recovery, moderate cooling, and the second recovery. The temperature values are expressed as means ± SD ($n = 6$). $^{*}p < 0.05$.

ing device surface temperature is 12.8 ± 2.8 °C), the temperature reductions further increased to 3.7 ± 3.2 °C, 3.9 ± 3.0 °C, 3.3 ± 2.5 °C and 2.5 ± 1.0 °C, respectively. Unlike the mild cooling situation, large standard deviations in the temperature reductions are found during the moderate cooling. Since our sample size is relatively small ($n = 6$), it is unclear whether the variation of the temperature reduction from one rat to another would have be decreased if a bigger sample size were used. One may simply interpret the observed results as an indication of the different blood flow and temperature responses to cooling in the rat group. Nevertheless, of note is that the cooling of the carotid arterial blood in the neck results in a significant reduction (p value is less than 0.05) in the temperature at all recording locations. Also, all temperatures recovered to the expected baseline values after termination of cooling. There were no significant differences between the recovered and the precooling baseline temperatures.

Fig. 6 shows a typical temperature change during the cooling and recovery processes. The illustrated temperature profiles are from the measured data of one rat. The figure indicates that the temperatures at all head locations decreased quickly when the mild cooling was initiated and steady states was established after about 30 min. The deeper the brain regions, the larger were the observed temperature reductions. Once the cooling was stopped, the temperatures increased immediately and recovered to their previous baseline values within approximately 15 min. Very similar trends were observed during the moderate CCA cooling; however, the recovery temperature was slightly higher than the baseline value, a finding (temperature rebound) similar to our previous experimental study on rats using head surface cooling and likely explained by rewarming "mismatch" between blood perfusion and brain metabolism [14].

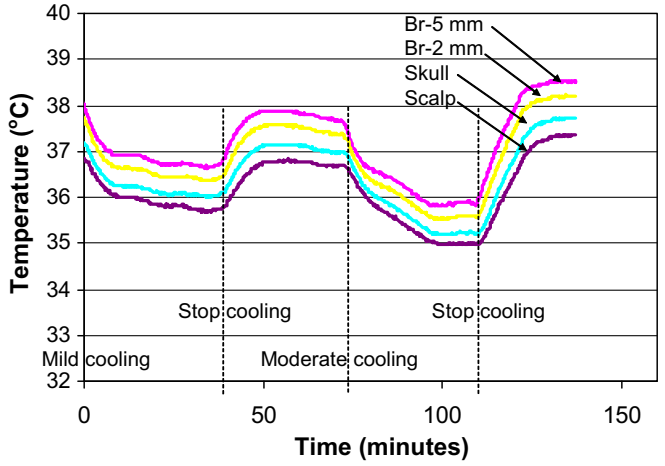

Fig. 6. Typical temperature transients during cooling and rewarming at various tissue locations.

The physical and physiological properties used in the theoretical simulation are listed in Table 2 and can be found in previous publications [10,19,21,22]. The average blood perfusion rate of the brain tissue, ω_{bt}, was not measured directly; however, a good correlation exists between the perfusion rate and measured CCA blood flow rate and the brain weight of the rat. From Diao [23], the ratio of the blood flow in the internal carotid artery to the total blood flow in the common carotid artery ($Q_{internal}/Q_{total}$) is equal to 0.56 in rats. Therefore, the average blood perfusion rate of the rat brain tissue, ω_{bt}, can be calculated by:

$$\omega_{bt} = Q_{internal}/M_{bt} = 0.56 \cdot Q_{total}/M_{bt} = 0.56 \cdot (Q_L + Q_R)/M_{bt} \quad (4)$$

where Q_L and Q_R are the blood flow rates (ml min^{-1}) measured in the left and right common carotid arteries, respectively, and M_{bt} is the mass (g) of the rat brain tissue measured immediately after each experiment. Assuming no significant difference in the blood flow rate between the left and right common carotid arteries and a constant,Q, the average blood perfusion rate of the brain tissue, ω_{bt}, can be obtained by:

$$\omega_{bt} = 1.12 \cdot Q/M_{bt} \quad (5)$$

Note that the unit of the blood perfusion rate calculated from Eq. (5) is ml min^{-1} g^{-1}, which is widely used in medical and biological research. In this study, the unit of ω in Eqs. (2) and (3) is s^{-1}. Therefore, the calculated values from Eq. (5) need to be converted to the required unit of s^{-1}, and they are listed in Table 2. We also assumed that the blood perfusion rate of the brain tissue did not significantly change during the cooling and rewarming periods. The metabolic heat generation in the tissue was determined based on the relationship between blood perfusion rate and metabolism as described elsewhere [22].

Table 3 provides the baseline combinations of the parameters used in the theoretical simulation. Most were determined from the average results of the data measured in the current experiments. The rat head is approximately 15 mm in radius and both the skin and skull layers are 1 mm in thickness. The rat neck is 16.5 mm in radius and is 20 mm in length. The average size of the common carotid artery is 1.5 mm in diameter, and it is located approximately in the middle between the cylinder center and the skin surface. The calculated average blood flow velocity of the carotid artery is 4.15 cm s^{-1}. Substituting the geometry parameters and thermal properties into the theoretical model, we obtained the steady state temperature distribution in the neck model. Fig. 7 illustrates the simulated steady state temperature decay along the common carotid artery for the mild or moderate cooling. It is a highly approximation that the temperatures of the major arteries do not deviate significantly from the tissue temperature at the center of the body [24]. The measured rat rectal temperature (38.3 °C) was, therefore, used as the temperature of the carotid

Table 2
Physical and physiological properties under normal conditions

	Specific heat c (J kg^{-1} K^{-1})	Mass density ρ (kg m^{-3})	Thermal conductivity k (W m^{-1} K^{-1})	Perfusion rate ω (ml min^{-1} 100 g) or (s^{-1})	Metabolic rate q_m (W m^{-3})
Blood	3800[a]	1050[c]	0.5[c]	–	–
Neck	3700[b]	1050[c]	0.5[c]	1.0 (0.000167)[d]	180.2[d]
Scalp	4000[a]	1000[c]	0.34[c]	2.0 (0.000333)[d]	363.4[d]
Bone	2300[a]	1500[c]	1.16[c]	1.8 (0.0003)[d]	368.3[d]
Brain tissue	3700[a]	1050[c]	0.5[c]	239.2 (0.0399)[e]	49937[e]

[a] Xu et al. (1999).
[b] Bommadevera and Zhu (2002).
[c] Olsen et al. (1985).
[d] Diao et al. (2003).
[e] Calculated from the animal experiments.

Table 3
Parameters of the baseline design

Head	Geometry	$r_1 = 13$ mm, $r_2 = 14$ mm, $r_3 = 15$ mm[d]
Cooling device	Geometry	10 mm long × 10 mm wide × 1 mm thick
	Location in the neck	0.25 mm from the carotid artery
	Surface temperature	18.7 °C or 12.8 °C at the outer surface of the device
Neck cylinder	Geometry	33 mm in diameter and 20 mm long
Carotid artery	Geometry	1.5 mm in diameter and 20 mm long
	Location in neck	$d = 2.5$ mm, $e = 8$ mm
	Flow rate	4.4 ml/min in each carotid artery
	Flow velocity	$u_a = 4.15$ cm s^{-1}

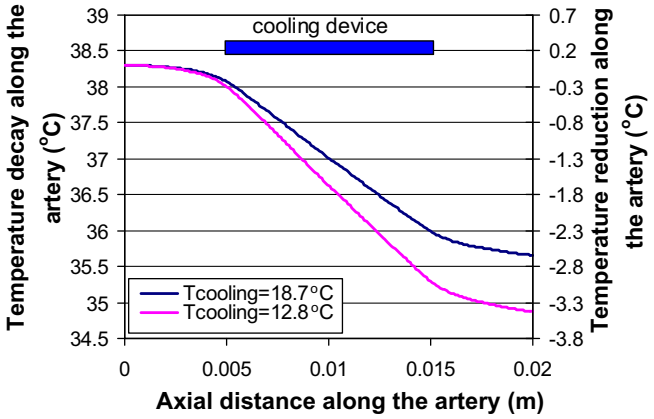

Fig. 7. Simulated temperature decays along the common carotid artery during cooling.

arterial blood at its entrance. At a higher device temperature of 18.7 °C, the simulated temperature decay along the artery was 2.6 °C (see the right *y*-axis in Fig. 7). When the device temperature was further decreased to 12.8 °C, the temperature reduction along the blood vessel increased accordingly to 3.4 °C.

Based on the simulated temperature at the terminus of the common carotid artery, T_{bm} in Eq. (3) was assigned as 35.7 °C and 34.9 °C for the mild and moderate cooling, respectively. Substituting the calculated arterial temperature into the brain model, we solved for the temperature fields in the head region. Figs. 8 and 9 provide the simulated steady state temperature distributions (lines) and the experimentally obtained measurements (symbols) at the four monitored sites. Again, the large standard deviations

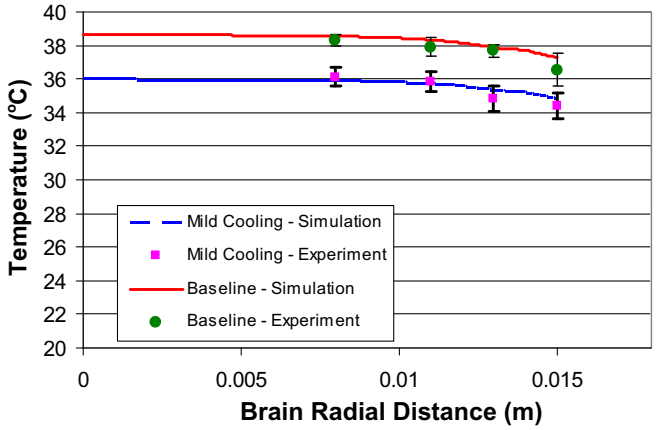

Fig. 8. Theoretically predicted radial temperature distribution (lines) and experimental measurements (symbols) during steady state for the mild cooling.

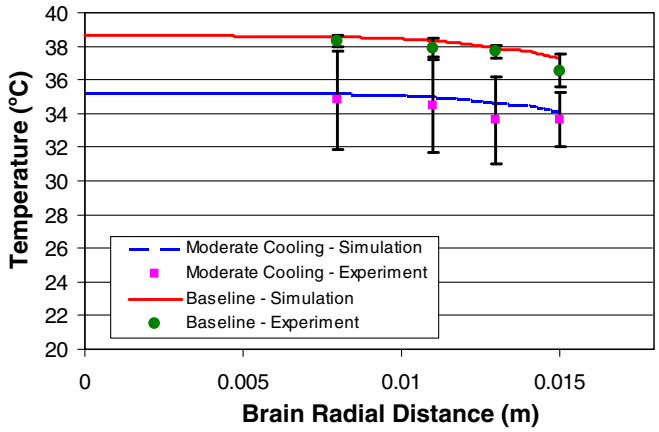

Fig. 9. Theoretically predicted radial temperature distribution (lines) and experimental measurements (symbols) during steady state for the modest cooling.

in Fig. 9 are from the experimental measurements. In the theoretical study, we only simulate the temperature fields based on the average values of the experimental parameters. A good agreement between the theoretical simulation predictions of the temperature trends and the experimental results was found.

5. Discussion and conclusions

In this study, we assumed that the average blood perfusion rate of the brain tissue, ω_{bt}, is proportional to the average blood flow rate in the common carotid artery. It is not clear whether the ratio of internal-to-external carotid artery blood flow, that is, the blood shunted to the brain tissue or external head, respectively, changes during either cooling or rewarming. However, a previous investigation by our group [14] had delineated similar dynamics of temperature responses in the brain tissue temperature and the CCA flow rate when the blood flow was continuously monitored; therefore, the CCA flow rate seems to be a reasonable index of the blood perfusion in the brain tissue. Further, during the experiments, the flow rates of both CCA were measured exclusively during the baseline period, and in our theoretical simulation we assumed those to remain constant during the cooling process. Even though the CCA flow rate can be monitored during the cooling [14], we felt that having a flow meter (~5 mm) in place during the cooling periods would interfere with accurate cooling induction in the neck tissue. Similarly; non-invasive brain perfusion measurement approaches, such as laser Doppler or MRI, have inherent shortcomings (i.e., regional flow readings of laser Doppler devices) or are too impractical (real-time MR imaging) for continuous monitoring of the blood perfusion in brain tissue.

The possibility of significant changes in the CCA flow relates to uncertainty in the blood perfusion rate of brain tissue during cooling. Temperature fields in both the neck and head regions can then be affected. As shown in our previous theoretical simulation [18], temperature reductions along the common carotid artery were almost inversely proportional to its blood flow rate. Therefore, decreasing the blood flow rate by 50% would double the temperature drop along the artery. The total heat loss from the arterial blood to the cooling device can be written as $q_{loss} = 2\rho_b c_b\ Q\Delta T$, where Q is the volumetric flow rate and ΔT is the total temperature change along the blood vessel. Therefore, the total heat loss would not be very sensitive to the flow rate. This is expected since the total heat loss from the artery is determined by the thermal resistance in the cross-sectional plane in the neck cylinder [18,24]. Noted that the blood supply to the brain is originated from the common carotid as well as the posterior neck (vertebral) arteries,

mixed at the base of the skull (Circle of Willis). One may assume that any decrease or increase in the common carotid blood flow is compensated by an increase or decrease in the vertebrate blood flow. Since the objective of any hypothermia technique is to decrease the brain tissue temperature, the same amount of heat removed from the carotid arterial blood would eventually induce a corresponding temperature decrease in the brain tissue. Or, in other words, the inaccuracy of the value of the blood flow rate in the common carotid artery may not affect significantly the global temperature reduction in the brain, since the total heat loss from the arteries is almost independent of the blood flow rate in the arteries.

There are several limitations associated with the theoretical model due to the restriction of the computer software used in the study. The rat neck is not a pure cylinder and the brain is not exactly hemispherical. The spatial variations in the thermal properties and blood perfusion are not considered in the simulation. The top surface of the neck was prescribed as an adiabatic boundary condition, although heat loss between the head and neck regions remains uncertain. Our previous theoretical analyses in the human neck and head regions gave a heat flux of approximately 16 W m^{-2} after computational iterations. However, the heat loss from the interface was less than 0.2 W due to the small heat transfer area involved. The dominant mechanism of temperature reduction in the brain, therefore, is the arterial cooling along the common carotid arteries ($\sim$90 W in blood cooling in the human neck). The good agreement between the theory and experiment in this study therefore increases the credibility of our theoretical analyses.

Although targeted brain hypothermia is proposed to avoid well-documented systemic complications induced by whole-body cooling, cooling the brain alone may still affect the overall thermoregulation. It is well known that brain tissue is only 2% of the body weight; however, it requires more than 20% of the cardiac output. Cooling the adjacent jugular venous blood is inevitable using an interstitial cooling device in close proximity to the CCA; similarly, venous return from arterially cooled brain will influence the systemic blood temperature as well. Under the experimental circumstances; however, a heating pad was employed to maintain the animal's core temperature, which, in analogy, could be utilized in clinical setting as well.

In clinically employed brain cooling, one needs not only control the depth of cooling but also the speed of rewarming, since excessive rewarming of the injured brain commonly leads to a mismatch between cerebral metabolism and perfusion. The mismatch is interpreted as flow-metabolism uncoupling which can result in rebound intracranial pressure elevations, cerebral perfusion reductions, and brain ischemia. In the current study, rewarming was induced by ending coolant circulation in the cooling device. It led to a rewarming rate of more than 5 °C/h, which is much higher than the recommended cooling rate of 0.5 °C h^{-1} to minimize the adverse effects. Future developments of clinically employed cooling systems will necessarily utilize controlled temperature modes and will not be dependent on spontaneous brain rewarming as in our experiments. For example, a theoretical model could be used to predetermine the relationship between the temperature of the coolant and the brain tissue to control the rewarming rate.

In conclusion, we employed *in vivo* experiments on rats to evaluate the performance of a newly developed neck cooling device and its feasibility for rapid induction and maintenance of brain hypothermia. Good agreement between the theoretically predicted and experimentally obtained temperature distributions in the rat brain demonstrated the validity of a previously developed theoretical model for humans. The model is capable of correctly predicting heat transfer within the complicated vasculature in the neck and head regions. Simultaneously, euthermic body temperatures were maintained by active heating of the body, thereby reducing the impact of cooled venous return from the head. Inspections of the *in vivo* cooling sites did not indicate that the interstitial cooling device led to local, cold-induced tissues injuries. The current study is viewed as an important first step in developing a compact and reliable neck cooling device with a potential for future clinical development.

Acknowledgments

The authors are grateful to Drs. Olav Thulesius and Huan Wang for their helpful comments. Dr. Zhu thankfully acknowledges financial assistance by an NSF-supported UMBC ADVANCE program. Dr. Rosengart was supported in part by the Brain Research Foundation, The University of Chicago Medical Center, and the Cancer Research Foundation, Chicago, Illinois. The research was performed in partial fulfillment of the requirements for the Ph.D. degree from the University of Maryland Baltimore County by Yunjian Wang.

References

[1] G.W. Roach, M. Kanchuger, C.M. Mangano, M. Newman, N. Nussmeier, R. Wolman, A. Aggarwal, K. Marschall, S.H. Graham, C. Ley, Adverse cerebral outcomes after coronary bypass surgery. Multicenter Study of Perioperative Ischemia Research Group and the Ischemia Research and Education Foundation Investigators, New Eng. J. Med. 335 (1996) 1857–1863.
[2] J.H. Miller, Partial replacement of an infected arterial graft by a new prosthetic polytetrafluoroethylene segment: a new therapeutic option, J. Vasc. Surg. 17 (3) (1993) 546–558.
[3] N.A. Nussmeier, A review of risk factors for adverse neurological outcome after cardiac surgery, J Extra-Corporeal Technol. 34 (2002) 4–10.
[4] S. Levine, H. Payan, Effects of ischemia and other procedures on the brain and retina of the gerbil (*Meriones unguiculatus*), Exp. Neurol. 16 (3) (1966) 255–262.
[5] U.M. Illievich, M.H. Zornow, K.T. Choi, M.S. Scheller, M.A. Strnat, Effects of hypothermic metabolic suppression on hippocampal glutamate concentrations after transient global cerebral ischemia, Anesth. Analg. 78 (5) (1994).
[6] K.H. Polderman, Application of therapeutic hypothermia in the intensive care unit. Opportunities and pitfalls of a promising treatment modality. Part 2: Practical aspects and side effects, Intens. Care Med. 30 (2004) 757–769.
[7] S. Nurse, D. Corbett, Direct measurement of brain temperature during and after intraischemic hypothermia: correlation with behavioral, physiological, and histological endpoints, J. Neurosci. 14 (12) (1994) 7726–7734.
[8] H. Minamisawa, C.H. Nordstrom, M.L. Smith, B.K. Siesjo, The influence of mild body and brain hypothermia on ischemic brain damage, J. Cerebr. Blood Flow Metab. 10 (3) (1990) 365–374.
[9] D.W. Marion, L.E. Penrod, S.F. Kelsey, W.D. Obrist, P.M. Kochanek, A.M. Palmer, S.R. Wisniewski, S.T. DeKosky, Treatment of traumatic brain injury with moderate hypothermia, New Eng. J. Med. 336 (1997) 540–546.
[10] C. Diao, L. Zhu, H. Wang, Cooling and re-warming for brain ischemia or injury: theoretical analysis, Ann. Biomed. Eng. 31 (2003) 346–352.
[11] L. Zhu, C. Diao, Theoretical simulation of temperature distribution in the brain during mild hypothermia treatment for brain injury, Med. Biol. Eng. Comput. 39 (2001) 681–687.
[12] M. Allers, F. Boris-Moller, A. Lunderquist, T. Wieloch, A new method of selective rapid cooling of the brain: an experimental study, Cardiovasc. Intervent. Radiol. 29 (2006) 260–263.
[13] M.R. Battin, J. Penrice, T.R. Gunn, A.J. Gunn, Treatment of term infants with head cooling and mild systemic hypothermia (35.0 °C and 34.5 °C) after perinatal asphyxia, Pediatrics 111 (2003) 244–251.
[14] C. Diao, L. Zhu, Temperature distribution and blood perfusion response in rat brain during selective brain cooling, Med. Phys. 33 (7) (2006) 2565–2573.
[15] H. Wang, G. Olivero, W. Lanzino, J. Elkins, D. Rose, M. Honings, M. Rodde, J. Burnham, D. Wang, Rapid and selective cerebral hypothermia achieved using a cooling helmet, J. Neurosurg. 100 (2004) 272–277.
[16] L. Zhu, A.J. Rosengart, Cooling penetration into normal and injured brain via intraparenchymal brain cooling probe: theoretical analyses, Heat Transfer Eng. 29 (3) (2008) 284–294.
[17] L. Zhu, Theoretical evaluation of contributions of both radial heat conduction and countercurrent heat exchange in selective brain cooling in humans, Ann. Biomed. Eng. 28 (2000) 269–277.
[18] Y. Wang, L. Zhu, Selective brain hypothermia induced by an interstitial cooling device in human neck: theoretical analyses, Eur. J. Appl. Physiol. 101 (2007) 31–40.

[19] M. Bommadevera, L. Zhu, Temperature difference between the body core and the arterial blood supplied to the brain during hyperthermia or hypothermia in humans, Biomech. Model. Mechanobiol. 1 (2) (2002) 137–149.
[20] H.H. Pennes, Analysis of tissue and arterial blood temperatures in the resting human forearm, J. Appl. Physiol. 1 (1948) 93–122.
[21] R.W. Olsen, L.J. Hayes, E.H. Wissler, H. Nikaidoh, R.C. Eberhart, Influence of hypothermia and circulatory arrest on cerebral temperature distributions, ASME J. Biomech. Eng. 107 (1985) 354–360.
[22] X. Xu, P. Tikuisis, G. Giesbrecht, A mathematical model for human brain cooling during cold-water near-drowning, J. Appl. Physiol. 86 (1999) 265–272.
[23] C. Diao, A numerical and experimental study on temperature distribution and blood flow response in the brain during selective brain cooling, Ph.D. dissertation, University of Maryland Baltimore County, 2004.
[24] S. Weinbaum, L.M. Jiji, D.E. Lemons, Theory and experiment for the effect of vascular microstructure on surface tissue heat transfer – Part I: Anatomical foundation and model conceptualization, ASME J. Biomech. Eng. 106 (1984) 321–330.